

Influence of Terrain Slope on Sub-Surface Fire Behavior in Boreal Forests of China

Yanlong Shan ^{1,*}, Bo Gao ¹, Sainan Yin ¹, Diankun Shao ², Lili Cao ¹, Bo Yu ¹, Chenxi Cui ¹ and Mingyu Wang ^{3,*}

¹ Science and Technology Innovation Center of Wildland Fire Prevention and Control of Beihua University, Forestry College, Beihua University, Jilin 132013, China

² Jilin Institute of Land and Resources Investigation and Planning, Changchun 130012, China

³ Ecology and Nature Conservation Institute, Chinese Academy of Forestry, Beijing 100091, China

* Correspondence: shanyl@ustc.edu.cn (Y.S.); fire@caf.ac.cn (M.W.)

Abstract: In recent years, the influence of extreme weather patterns has led to an alarming increase in the frequency and severity of sub-surface forest fires in boreal forests. The *Ledum palustre-Larix gmelinii* forests of the Daxing'an Mountains of China have emerged as a hotspot for sub-surface fires, and terrain slope has been recognized as a pivotal factor shaping forest fire behavior. The present study was conducted to (1) study the effect of terrain slope on the smoldering temperature and spread rate using simulated smoldering experiments and (2) establish occurrence probability prediction model of the sub-surface fires' smoldering with different slopes based on the random forest model. The results showed that all the temperatures with different slopes were high, and the highest temperature was 947.91 °C. The spread rates in the horizontal direction were higher than those in the vertical direction, and the difference increased as the slope increased. The influence of slope on the peak temperature was greater than that of spread rate. The peak temperature was extremely positively correlated with the slope, horizontal distance and vertical depth. The spread rate was extremely positively correlated with the slope. The spread rate in the vertical direction was strongly positively correlated with the depth, but was strongly negatively correlated with the horizontal distance; the horizontal spread rate was opposite. The prediction equations for smoldering peak temperature and spread rate were established based on slope, horizontal distance, and vertical depth, and the model had a good fit ($p < 0.01$). Using random forest model, we established the occurrence prediction models for different slopes based on horizontal distance, vertical depth, and combustion time. The models had a good fit (AUC > 0.9) and high prediction accuracy (accuracy > 80%). The study proved the effect of slope on the characteristics of sub-surface fire smoldering, explained the variation in peak temperature and spread rate between different slopes, and established the occurrence prediction model based on the random forest model. The selected models had a good fit, and prediction accuracy met the requirement of the sub-surface fire prediction.

Keywords: boreal forests; Daxing'an Mountains; peak temperature; random forest model; slope; spread rate; sub-surface fires



Citation: Shan, Y.; Gao, B.; Yin, S.; Shao, D.; Cao, L.; Yu, B.; Cui, C.; Wang, M. Influence of Terrain Slope on Sub-Surface Fire Behavior in Boreal Forests of China. *Fire* **2024**, *7*, 55. <https://doi.org/10.3390/fire7020055>

Academic Editor: Grant Williamson

Received: 22 December 2023

Revised: 1 February 2024

Accepted: 9 February 2024

Published: 14 February 2024



Copyright: © 2024 by the authors. Licensee MDPI, Basel, Switzerland. This article is an open access article distributed under the terms and conditions of the Creative Commons Attribution (CC BY) license (<https://creativecommons.org/licenses/by/4.0/>).

1. Introduction

Global warming and increased human activities in recent years have led to a rise in the frequency and severity of forest fires within boreal ecosystems [1]. Forest fires encompass surface fires, canopy fires, and sub-surface fires. Even though sub-surface fires occur less frequently compared to canopy or surface fires, their impact is substantial [2]. Sub-surface fires typically occur within the humus or peat layer [3]. These fires are characterized by low temperatures, a lack of flames, and slow smoldering spread. The primary source of fuel for sub-surface fires are plant roots and the organic carbon content within the soil; thus, sub-surface fires can lead to adverse effects, including soil structure degradation, widespread plant mortality, and the release of numerous particles and pollutant gases [4].

The peat fires in Indonesia during 1997 and 1998 released 0.95 Gt of CO₂, which was equivalent to 15% of global human fossil carbon emission for the same period [5]. Coniferous forests located in boreal forests are a hot spot for sub-surface fires [6]. Prolonged fire seasons and increased permafrost melting have significantly increased the risk of sub-surface fires in boreal forests [7,8]. Therefore, the study of sub-surface fire occurrence and fire behavior is important to predict the occurrence and spreading mechanism of sub-surface fires. However, literature on sub-surface fires is scarce. Most of the studies in this field are directed mainly towards peat fires [9–11], and only few studies are on fires in humus layers [12,13]. Oxygen content, fuel density, moisture content of fuel, terrain, and meteorological conditions are considered to be the important factors affecting the fire behavior [14–17]. The slope of the terrain is a main topographic factor that can affect the occurrence and spreading of sub-surface fires. The slope can affect the occurrence of forest fires by influencing the distribution of fuel and moisture content [18,19]. Further, slope can affect the spread of forest fire by changing the way of radiative and convective heat transfer during the spread [20,21]. Studies on the effect of slope on forest fire behavior mainly focus on the surface fire behavior [22–25]. However, due to differences in fuel types and heat transfer modes, there are significant differences in the combustion temperature, spread rate, and other fire behaviors between surface fire and sub-surface fire [17,26]. The effect of slope on sub-surface fire behavior is rarely reported. Existing fire prediction models are based on the indirect factors and traditional generalized linear models [27–29], and the applicability and accuracy of these models are very low. In recent years, machine learning has become the main method of forest fire occurrence prediction due to its high accuracy, low overfitting risk, and high tolerance for data outliers [30]. The random forest model in particular is widely used in forest fire occurrence prediction [31–34], mapping wildfire-prone areas [35–37], and origin of fire and fire site identification [38–40]. Although the research on sub-surface fires has been developing, the prediction mechanism of sub-surface fire occurrence and the factors affecting of sub-surface fire behavior are still unclear.

Sub-surface fires mainly spread by radiation heat transfer and can occur with low oxygen content [26]. Therefore, the existing mechanism explaining the influence of slope on the surface fire behavior cannot be used to describe the sub-surface fire behavior. According to occurrence and spread characteristics, determining the location of sub-surface fires and the use of large machinery or manual excavation of inclined trench-shaped fire belts to cut off the fire line are important methods to prevent and extinguish sub-surface fires [4,41,42].

In recent years, many countries have reported the occurrence and harm of forest sub-surface fires. Based on the research on the behavior and influencing factors of sub-surface fires, establishing prediction models for the occurrence of sub-surface fires can more accurately determine the location and spread trend of sub-surface fires, and then develop targeted monitoring and suppression plans. This can not only effectively block the spread path of sub-surface fires, but also ensure the safety of firefighters [41,43]. This research is focused on the *Ledum palustre-Larix gmelinii* forest in the Daxing'an Mountains, which is prone to sub-surface fires. The objectives of the present study were to: (1) quantify the characteristics of sub-surface fire behavior under different slopes; (2) identify the influence of slope on sub-surface fire behavior; and (3) establish an occurrence prediction model of sub-surface fires through simulated smoldering experiments, in order to explain the factors affecting sub-surface fire behavior.

2. Materials and Methods

2.1. Study Site

The study area was located in Huzhong National Nature Reserve (HNNR) in the Daxing'an Mountains, China (122°42'14"–123°18'05" E, 51°17'42"–51°56'31" N). This region has a cold temperate continental monsoon climate, with an annual average temperature of −4 °C and annual precipitation of 395–688 mm. The forest vegetation type is cold and warm coniferous forest, which is a continuation of the southward distribution of the bright coniferous forests of Siberia. *Larix gmelinii* is the dominant species, and the main tree

species include *Betula platyphylla*, *Populus davidiana*, *Pinus sylvestris* var. *mongolica*, and *Chosenia arbutifolia*. The main understory vegetation includes *Ledum palustre*, *Rhododendron dauricum*, and *Pinus pumila*. Sub-surface forest fires in this region (Figure 1) are mostly caused by surface fires from lightning [44]. Thus, frequent lightning fires in HNNR create conditions for sub-surface fires.



Figure 1. Sub-surface fires in Huzhong National Nature Reserve: (a) smoldering phenomenon of sub-surface fires; (b) trees affected in sub-surface fires.

2.2. Sampling and Processing of Humus

The study is focused on the *Ledum palustre-Larix gmelinii* forest which is the hotspot for sub-surface fires in HNNR. Three sample plots were randomly selected, and three sets of 50 cm × 50 cm quadrats each were established diagonally on the 3 sample plots. All the ground fuels of the quadrats were collected and transported to the laboratory (Figure 2). Samples of humus were placed in archival paper bags and dried at 105 °C for 48 h in a drying oven. Moisture contents were measured from 3 samples prior to the smoldering experiment using a rapid moisture monitor, with the average value being used as the experimental moisture content of the samples.

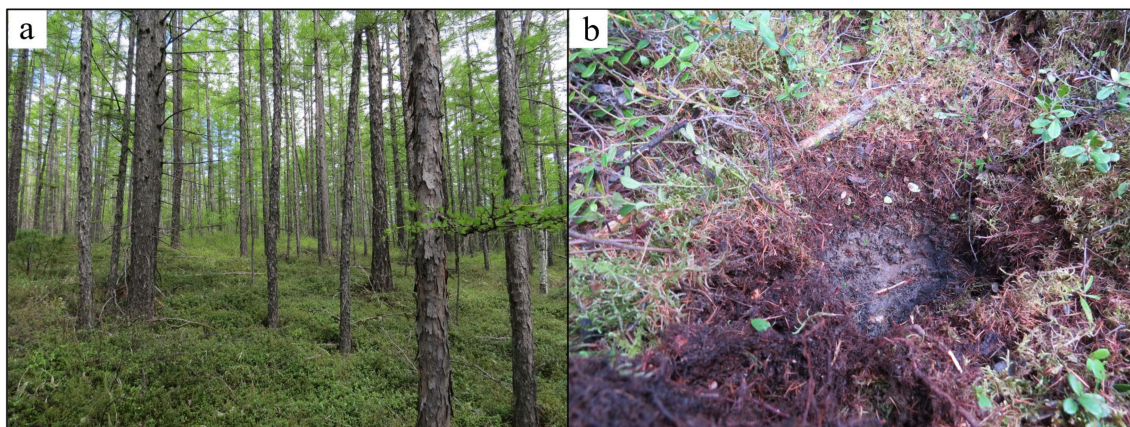


Figure 2. Sampling site: (a) *Ledum palustre-Larix gmelinii* forest vegetation; (b) 50 cm × 50 cm pit with exposed humus layer.

2.3. Simulating Smoldering Experiment

Simulating smoldering experiments were conducted using a self-assembled sub-surface fire temperature acquisition system consisting of a smoldering furnace, thermocouple, data acquisition module, far-infrared heating plate, and laptop. The smoldering furnace was cuboid in shape and made of aluminosilicate fiber material, which provided good insulation. The data acquisition module comprised a 16-channel NI9213 voltage acquisition board and a DAQ-9174 chassis (4 card slots), both produced by NI Corporation

in the United States. This module was capable of achieving real-time synchronous data transmission with a temperature measurement accuracy of $<0.25\text{ }^{\circ}\text{C}$. The data collection software utilized LabVIEW 2018, which could directly convert electrical signals into temperature data. Forty-five holes (5 vertical and 9 horizontal) with a diameter of 2 mm each were drilled with 3 cm gaps on the side of the cuboid furnace. As the majority of the Daxiing'an Mountains are gentle slopes [45], three slope angles (0° , 10° and 20°) were selected. Fuels were put into the smoldering furnace separately. A type K thermocouple was inserted into the middle of the humus through the drilled holes. One side of the furnace was lifted, and the slopes were set using an inclinometer. The far-infrared heating plate was placed over the smoldering furnace, and the heating temperature was set at $500\text{ }^{\circ}\text{C}$. The power supply was disconnected after heating for 0.5 h. The thermocouples and data acquisition module were connected by compensation wires, and the temperature variation data of the humus combustion were transmitted back to the laptop at 1 min intervals. The experiment was repeated 3 times for each slope (Figure 3).

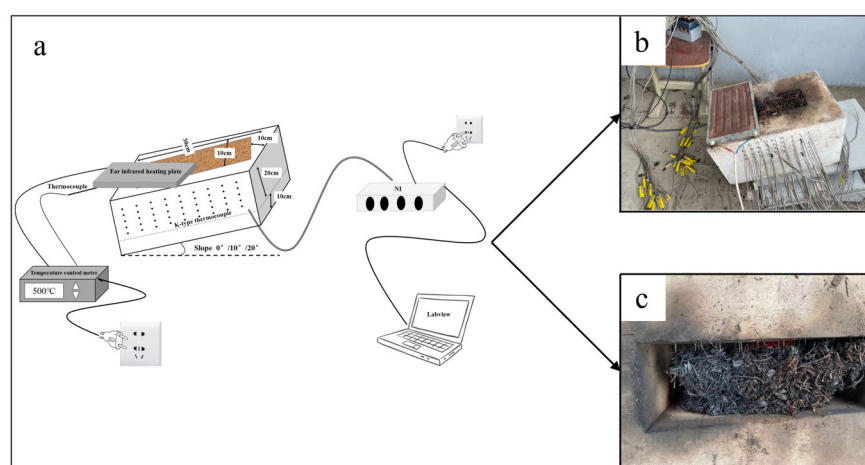


Figure 3. The simulating smoldering experimental setup: (a) schematic diagram of the experimental setup; (b) the simulating ignition experimental; (c) the ground fuel smoldering.

2.4. Data Processing and Analysis

The spread rates in the vertical direction (depth of the thermocouple/combustion time to the peak temperature) and horizontal direction (distance of the thermocouple/combustion time to the peak temperature) were recorded and analyzed. The effects of slope on the peak temperature and spreading rate in the vertical and horizontal directions were analyzed by the variance analysis method. Multiple comparisons were carried out using the least significant difference (LSD) test. Correlation analysis and regression analysis were used to analyze the relationship between peak temperature, spread rate, and slope, vertical depth, horizontal distance, and prediction models were established.

Using the horizontal distance, vertical depth, and combustion time of smoldering as independent variables, the occurrence probability prediction models on different slopes were established based on a random forest model. These models obtained 'm' sample sets by randomly conducting 'm' number of random replacement samplings from the training samples and building the tree predictors. The final classification results were divided by multi-tree voting.

When the combustion temperature of sub-surface fires is higher than $300\text{ }^{\circ}\text{C}$, obvious smoldering will occur, and carbon will be pyrolyzed [46]. Therefore, when the smoldering temperature was $\geq 300\text{ }^{\circ}\text{C}$, it was recorded as 1; otherwise, it was regarded as not smoldering and recorded as 0. The respective occurrence probability prediction models of different slopes were established. Before establishing the models, the data were divided into 60% training samples and 40% validation samples. The training samples were used to establish the prediction models, and the validation samples were used to verify the accuracy of the models.

The area value (AUC) under the receiver operating characteristic (ROC) curve was used as the evaluation criterion of the fitting degree. The Youden index was calculated according to the abscissa (1-specificity) and ordinate (sensitivity) of the ROC curve. The larger the Youden index, the higher the true positive rate and true negative rate of the model, and the more accurate the model's prediction. The cut-off value of the model was determined according to the maximum of the Youden index of the training samples, and the accuracy of the validation samples was calculated. The Youden index is as follows:

$$\text{Youden index} = \text{sensitivity} + \text{specificity} - 1$$

3. Results

3.1. Characteristics of Sub-Surface Fire Smoldering under Different Slopes

The sub-surface fire smoldering of the *Ledum palustre-Larix gmelinii* forest under different slopes was slow (Figure 4). In the early period of the smoldering, the smoldering temperatures were relatively low. With the development of sub-surface fire, smoldering gradually stabilized and temperatures gradually increased. Higher temperatures were mainly concentrated in the later period, and the temperatures in deep layers were significantly higher than those near the surface layer. When the slope was 0°, the temperatures mainly ranged from 220 to 620 °C, and the highest temperature reached 769.02 °C. When the slope was 10°, the temperatures mainly ranged from 420 to 720 °C, and the highest temperature reached 880.69 °C. When the slope was 20°, the temperatures were much higher than those at 0° and 10°, the highest temperature reached 947.91 °C. The spread rates of sub-surface fires in the horizontal direction were higher than those in the vertical direction with different slopes. As the slope increased, the difference between the vertical and horizontal spread rates gradually increased. The fastest spread rates were recorded at 20° of slope with 6.50 cm/h in the vertical direction and 10.41 cm/h in the horizontal direction. When the slope was 0°, the vertical spread rate was 3.42 cm/h, and the horizontal spread rate was 5.94 cm/h.

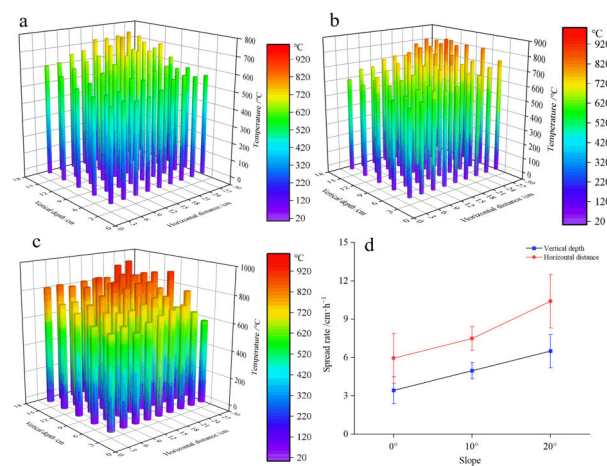


Figure 4. The characteristics of sub-surface fire smoldering under different slopes: (a) 0° slope; (b) 10° slope; (c) 20° slope; (d) Spread rate vs. slope.

3.2. Effect of Slope on Sub-Surface Fire Smoldering

The slope affected the peak smoldering temperature and spread rate in the vertical direction with different horizontal distances. With horizontal distances of 3–15 cm, the slopes had a significant influence on the peak smoldering temperature in the vertical direction (Figure 5a). The peak temperature of the 20° slope was significantly higher than the other two slopes. Within the horizontal distances of 18–27 cm, there was no difference between the peak temperatures of 10° and 20° slopes, but both were significantly higher than that of a 0° slope. The spread rates in the vertical direction had no significant difference with a horizontal distance of 3 cm. The spread rate of the 20° slope was the fastest with

the horizontal distance of 6–24 cm and showed a highly significant difference ($p < 0.01$) from that of the 0° slope (Figure 5b). The difference between 0° and 20° was less with a horizontal distance of 27 cm but still showed a significant difference ($p < 0.05$). The spread rate of the 10° slope had no significant difference from those of the 0° and 20° slopes.

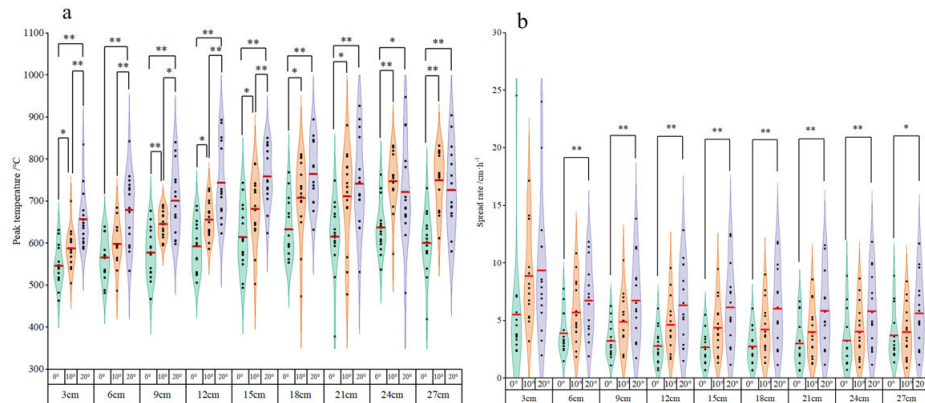


Figure 5. The influence of slope on (a) peak temperature and (b) spread rate of sub-surface fire smoldering in the vertical direction. Single asterisk (*) represents significant differences between treatments at $p < 0.05$; double asterisks (**) represent highly significant differences between treatments at $p < 0.01$. The dots in the figure represent data points of different treatments, and the red line represents the average value of the data points.

Slope had a significant influence on the peak temperature at all depths, and the peak temperature of the 20° slope was the highest, followed by the 10° slope, and that of the 0° slope was the lowest (Figure 6a). There were significant differences in peak temperatures among the three slopes (except for 12 cm), and the difference between the peak temperatures of the 20° and 10° slopes was lower than that of the 10° and 0° slopes at depths of 3–12 cm. The spread rate was the highest with the 20° slope, which was significantly higher than the other two slopes (except for the 3 cm depth) (Figure 6b). At the vertical depth of 3 cm, there were slight differences between the spread rates for different slopes. As the depth increased, the difference of the spread rates for different slopes increased in general. At the depth of 15 cm, there were significant differences among the three slopes.

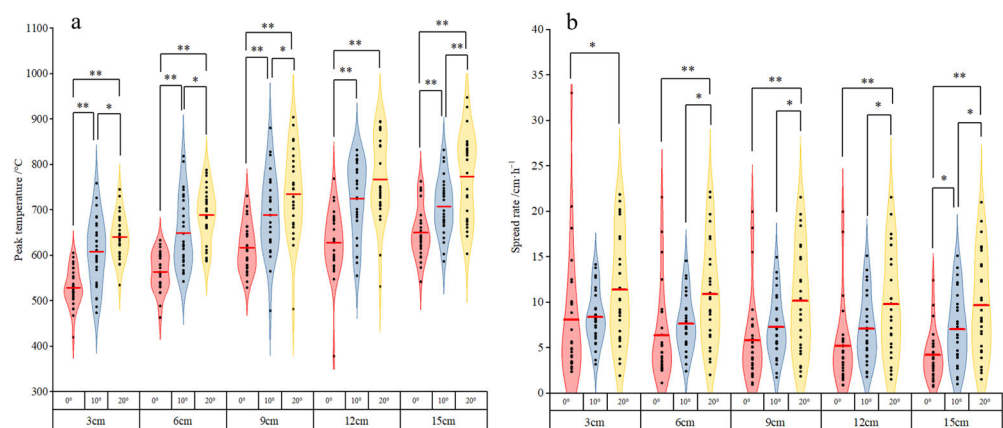


Figure 6. The influence of slope on (a) peak temperature and (b) spread rate of sub-surface fires in the horizontal direction. Single asterisk (*) represents significant differences between treatments at $p < 0.05$; double asterisks (**) represent highly significant differences between treatments at $p < 0.01$. The dots in the figure represent data points of different treatments, and the red line represents the average value of the data points.

The peak temperature had a significantly strong positive correlation with slope, vertical depth, and horizontal distance, indicating that the higher the slope, the greater the vertical depth, and the farther the horizontal spreading distance, the higher the smoldering temperature (Table 1). Spread rates in both the vertical and horizontal directions were positively correlated with slope. The spread rate in the vertical direction was positively correlated with the vertical depth and negatively correlated with the horizontal distance. The spread rate in the horizontal direction was negatively correlated with the vertical depth and positively correlated with the horizontal distance.

Table 1. Correlation analysis of smoldering characteristics of sub-surface fire with slope, vertical depth, and horizontal distance. Single asterisk (*) represents significant correlation between treatments at $p < 0.05$; double asterisks (**) represent highly significant correlation between treatments at $p < 0.01$.

Factors	Peak Temperature		Spread Rate in Vertical Direction		Spread Rate in Horizontal Direction	
	Correlation Coefficient	Sig.	Correlation Coefficient	Sig.	Correlation Coefficient	Sig.
Slope	0.511 **	<0.01	0.374 **	<0.01	0.351 **	<0.01
Vertical depth	0.444 **	<0.01	0.497 **	<0.01	−0.153 **	<0.01
Horizontal distance	0.339 **	<0.01	−0.239 **	<0.01	0.649 **	<0.01

The prediction equations of peak temperature and spread rate were established based on slope, vertical depth, and horizontal distance (Table 2). The three independent variables were highly significant ($p < 0.01$); thus the equation showed a good fit.

Table 2. The prediction models of the peak temperature and spread rate of the sub-surface fire smoldering.

Parameter	Independent Variable	Standard Error	Sig.	p-Value	Equation
Peak temperature	Constant	10.554	<0.01	<0.01	$y = 445.87 + 6.17x_1 + 10.31x_2 + 4.31x_3$
	Slope	0.394	<0.01		
	Vertical depth	0.759	<0.01		
	Horizontal distance	0.416	<0.01		
Spread rate in the vertical direction	Constant	0.412	0.01	<0.01	$y = 1.423 + 0.154x_1 + 0.394x_2 - 0.104x_3$
	Slope	0.015	<0.01		
	Vertical depth	0.030	<0.01		
	Horizontal distance	0.016	<0.01		
Spread rate in Horizontal distance	Constant	0.558	<0.01	<0.01	$y = 0.882 + 0.223x_1 - 0.187x_2 + 0.434x_3$
	Slope	0.021	<0.01		
	Vertical depth	0.040	<0.01		
	Horizontal distance	0.022	<0.01		

x_1 : Slope; x_2 : vertical depth; x_3 : horizontal distance.

3.3. The Occurrence Probability Prediction of Sub-Surface Fire Smoldering at Different Slopes

The random forest occurrence probability prediction models of sub-surface fire smoldering of different slopes were established based on the 3 independent variables, i.e., horizontal distance, vertical depth and combustion time, using the randomForest function in the R4.2.1 software program randomForest. The importance of the independent variable was calculated using the importance function. The variable importance of the 3 independent variables changed significantly with slopes (Table 3). The occurrence probability was most affected by the combustion time. This influence decreased with the increase in slope; however, the influence was still important overall. The second influential factor affecting the occurrence probability was horizontal distance. With increasing slope, the influence of the horizontal distance also increased. With a 20° slope, the horizontal distance was the most important variable instead of the combustion time. The third influential factor was vertical depth, and the effect of vertical depth decreased with increasing slope.

Table 3. The variable importance in the occurrence probability prediction models of sub-surface fire smoldering at different slopes.

Independent Variable	0°	10°	20°
Horizontal distance	32.91%	38.46%	53.80%
Vertical depth	32.12%	19.91%	14.02%
Combustion time	68.38%	51.98%	50.64%

The occurrence probability of the training and validation samples were calculated respectively by the predict function, and the ROC curves of prediction models for different slopes were drawn. The fitting effect of the 3 models was good, and the AUC values of the training sample and the validation sample could reach more than 0.9 (Figure 7). The fitting degree for 10° was the highest, and it was similar for 20° and 0°.

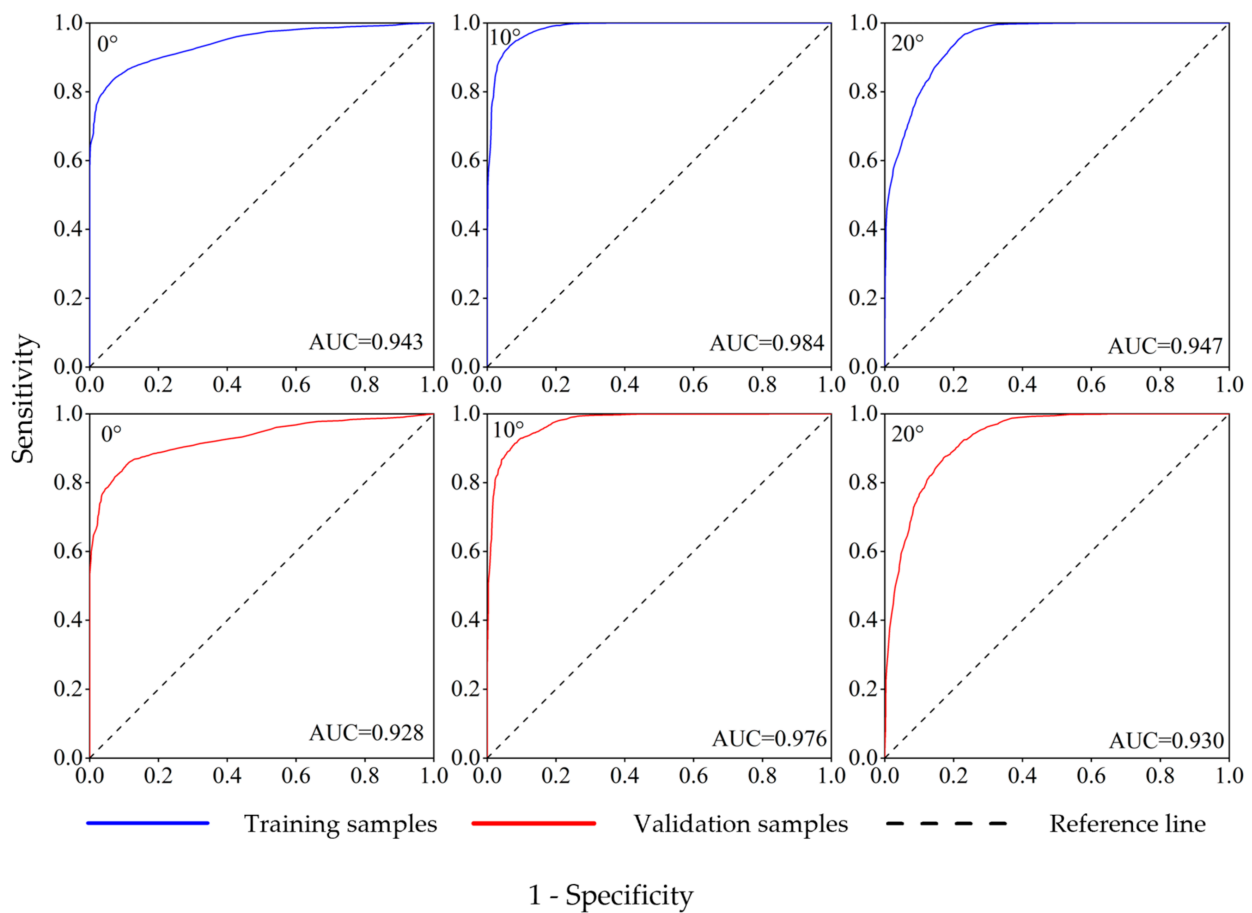


Figure 7. The ROC curves of the occurrence probability prediction models of different slopes.

Based on the Youden index, the cut-off values of the models selected for 0°, 10° and 20° slopes were 0.685, 0.605, and 0.235, respectively. The total accuracy of validation sample of the models of different slopes were >80% (Figure 8 and Table 4). The true negative rate of the models for 0° and 10° were above 90%, and the true positive rate of the models for 20° was above 90%. The accuracy sequence of the validation samples of the 3 models was 10° model > 0° model > 20° model, and the total accuracy was 91.54%, 85.95%, and 83.17%, respectively.

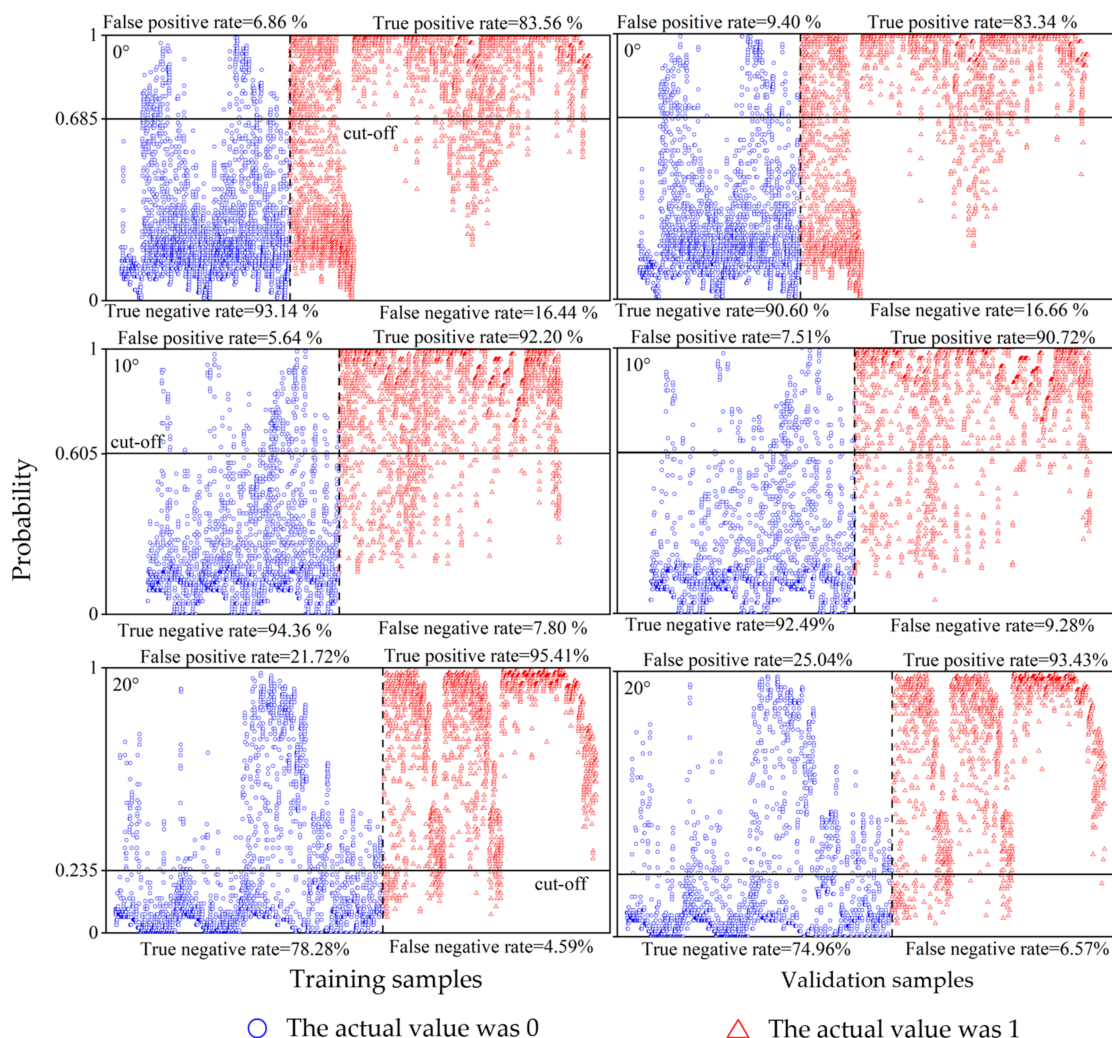


Figure 8. The accuracy evaluation of the occurrence probability prediction models of sub-surface fire smoldering for different slopes.

Table 4. The total accuracy of the validation samples of the occurrence probability prediction models of sub-surface fire smoldering for different slopes.

Slope	Smoldering/No Smoldering	Correct Forecast	Sample Size	Total Accuracy
0°	No smoldering	3336	3682	85.95%
	Smoldering	5461	6553	
10°	No smoldering	2806	3034	91.54%
	Smoldering	3187	3513	
20°	No smoldering	2093	2792	83.17%
	Smoldering	2089	2236	

4. Discussion

In this study, the characteristics of sub-surface fire smoldering of different slopes in the boreal forests of China were explained through ex situ simulated smoldering experiments. Compared with previous studies based on microscopic or small-scale experiments [15,47], the experimental scale of this study was larger. The sub-surface fire could spread both horizontally and vertically [48], while most studies have been carried out only in the vertical direction [13,17,49]. The present study simultaneously monitored and recorded the smoldering process in both the vertical and horizontal directions with an experimental cuboid furnace. Therefore, the three-dimensional smoldering process of the actual sub-

surface fire could be reflected accurately. The purpose of the simulation experiment was to get as close to a real fire as possible, and the larger the experiment scale, the more representative the data. Although the data of the smoldering process in this study are complex, and there might be some uncertainties in the experiment, the results will be useful for research on influential factors of sub-surface fire behavior and would also provide references for larger scale smoldering experiments.

The present study found that while the smoldering processes of different slopes were almost the same, the early smoldering was unstable, and the smoldering temperatures were relatively low. With the development of the sub-surface fire, the smoldering gradually stabilized, and the temperatures also gradually increased. When the slope was 20°, the highest temperature could reach 947.91 °C, while the peak temperatures in peat smoldering experiments were reported to be about 450–700 °C [50,51]. This indicated that the humus smoldering was different from the peat smoldering, and the damage to vegetation and the risk during fire extinguishing could be higher. The temperatures near the surface layers were lower than those in deep layers, as the sub-surface fires were sustained by the heat released from smoldering [52]. The heat in the surface layers was lost quickly, so the smoldering temperature was low. This would also lead to inadequate combustion in the surface layers. During the experiment, we found that, although smoldering had been sustained for a long time, the humus in the surface had not changed much. This may have been due to the insufficient smoldering in the surface layers. Therefore, there would have been a period for an overhanging phenomenon, which was consistent with Huang et al. [2]. This also reflects the hidden danger of sub-surface fires. The spread rates of the sub-surface fire of different slopes were faster in the horizontal direction, which was consistent with Graham et al. [53], indicating that the spread of smoldering first took place horizontally and then in a downward direction. A reasonable explanation for this phenomenon is that, although flame is absent in sub-surface fires, the surface temperature above the smoldering zone is higher. When there is no slope, heat is dissipated upwards. However, when the slope increases, it causes hot air to flow upwards along the surface of the fuel, thereby accelerating the drying and preheating process of the unburned fuel. This creates more favorable spreading conditions, leading to an increase in the horizontal spread rate. With the increase of the slope, the difference between spread rates in horizontal and vertical directions also increases. Therefore, it could be inferred that when a slope is steeper, the spread rate in the horizontal direction might be higher, and the fire is more likely to spread to the surface. However, this hypothesis must be further studied and verified.

Slope was considered an important factor affecting surface fire behavior [54], and this study found that slope also affects sub-surface fire behavior. The sub-surface fire behavior in the vertical direction was greatly affected by slope at the initial stage, and the dividing point of peak temperature was 15 cm in the horizontal direction. Davies [41] and Marcotte et al. [13] also indicated the critical conditions in the smoldering process. With the increase of horizontal distance during smoldering, the difference of peak temperatures and spread rates between different slopes decreased. With an 18 cm horizontal spread, there was no difference between the peak temperatures on 10° and 20° slopes. At different horizontal distances, there was no difference in spread rate between 10° and 20° slopes. This shows that once sub-surface fire smoldering begins, external conditions have difficulty influencing fire behavior. At different depths, the influence of slope on the peak temperature and spread rate in the horizontal direction were basically the same. There was a significant difference in peak temperatures between different slopes (except for 12 cm), and the difference between 0° and 10° was relatively smaller, but both were significantly lower than that of the 20° slope. Thus, the peak temperature was more affected by slope than the spread rate in both the vertical and horizontal directions. Pimont et al. [55] also found that the spread rate of surface fire changed weakly with the change of slope under low slope conditions.

The peak temperature of sub-surface fire smoldering indicated a strong positive correlation with slope, horizontal distance, and vertical depth. Huang et al. [2] also found that as smoldering spread progressed, the peak temperature increased. Steep slope

angles, high humus content in the upper soil layer, large collapse area, introducing a large amount of oxygen to deep layers, and high oxygen content could make smoldering more severe [15], resulting in high peak temperatures. With the increase of vertical combustion depth and horizontal distance, the vertical smoldering temperature was more stable due to the obstruction of surface fuel, resulting in the accumulation of heat in the horizontal direction. As mentioned above, smoldering was sustained by the heat that it released itself, so the peak temperature was positively correlated with both vertical depth and horizontal distance. The spread rates in the horizontal and vertical directions were strongly and positively correlated with the slope. Liu [56] and Rossa et al. [22] also pointed out that the spread rate of surface fire increased with the increasing slope, and extreme fire behavior would occur when the slope was too high. The role of sub-surface fire on extreme fire behavior with steeper slope conditions must be further studied in future research.

The prediction equations of the peak temperature and spread rate had good fitting with high prediction accuracy based on slope, vertical depth, and horizontal distance ($p < 0.01$), which would be helpful for sub-surface fire monitoring and warning. In recent years, with the development of computer technology, machine learning models such as random forest have been gradually employed in the study of forest fire occurrence prediction, and the prediction accuracy of these models has been shown to be higher than that of the traditional generalized linear models [57–59]. In this study, the random forest model was used in the occurrence probability prediction of sub-surface fire smoldering for the first time. According to the results, it could be inferred that the combustion time had a great influence on the occurrence probability. Strengthening the monitoring and warning ability regarding sub-surface fires and predicting or detecting the occurrence of sub-surface fire as early as possible is an important method to reduce sub-surface fire and forest resource loss. The influence of horizontal distance on the occurrence probability increased with the increase of slope, while the influence of vertical depth decreased with the increase of slope. It could be seen that the ability of smoldering to overcome the resistance caused by slope and to continue to spread forward is the key in determining whether sub-surface fires will occur or not. Due to the strong concealment of sub-surface fires, the research on the occurrence prediction are scarce. According to our study, it was shown that random forest model could be applied to the occurrence prediction of sub-surface fires. The machine learning methods also include support vector machine, neural networks, and other methods [60,61]. In the follow-up study, we are planning on using more algorithms and variables to improve the research about the prediction of sub-surface fires.

5. Conclusions

This study determined the influence of slope on the characteristics of sub-surface smoldering, and established the occurrence probability prediction model. The smoldering temperature was higher under different slopes, especially in the deep layers. The maximum smoldering temperature could reach 947.91 °C when the slope was 20°. The spread rate in the horizontal direction was higher than the vertical direction, and the difference increased with the increase of the slope. The influence of slope on the peak temperature of sub-surface smoldering was greater than the spread rate. The peak temperature showed a strong positive correlation with slope, horizontal distance, and vertical depth. The spread rates in the horizontal and vertical directions showed a strong positive correlation with slope. The spread rate in the vertical direction showed a strong positive correlation with the vertical depth and negatively correlated with the horizontal distance, while the horizontal spread rate was opposite. The prediction models based on the random forest model had good fitting effect ($AUC > 0.9$), and high accuracy. The total prediction accuracy of the validation sample was above 80%. The findings of this study expanded the factors known to contribute to sub-surface fire smoldering, and supported the research on prediction models for sub-surface fire occurrence.

Author Contributions: Conceptualization, Y.S., S.Y. and B.G.; methodology, M.W. and Y.S.; software, B.G. and S.Y.; validation, Y.S. and M.W.; formal analysis, Y.S., B.G. and S.Y.; investigation, D.S., S.Y., B.G., L.C., B.Y. and C.C.; resources, Y.S.; data curation, S.Y.; writing—original draft preparation, S.Y. and B.G.; writing—review and editing, Y.S. and B.G.; visualization, S.Y. and B.G.; supervision, Y.S.; project administration, Y.S.; funding acquisition, Y.S. All authors have read and agreed to the published version of the manuscript.

Funding: This research was funded by the National Key R&D Program of China (Grant 2023YFD2202004), and the National Natural Science Foundation of China (Grant Nos. 31971669, 32271881).

Institutional Review Board Statement: Not applicable.

Informed Consent Statement: Not applicable.

Data Availability Statement: The data presented in this study are available upon request from the corresponding authors.

Acknowledgments: We thank the Forestry College of Beihua University for their support for this research.

Conflicts of Interest: The authors declare no conflicts of interest.

References

1. Dye, A.W.; Gao, P.; Kim, J.B.; Lei, T.; Riley, K.L.; Yocom, L. High-resolution wildfire simulations reveal complexity of climate change impacts on projected burn probability for Southern California. *Fire Ecol.* **2023**, *19*, 20. [[CrossRef](#)]
2. Huang, X.; Restuccia, F.; Gramola, M.; Rein, G. Experimental study of the formation and collapse of an overhang in the lateral spread of smouldering peat fires. *Combust. Flame* **2016**, *168*, 393–402. [[CrossRef](#)]
3. Mickler, R.A.; Welch, D.P.; Bailey, A.D. Carbon emissions during wildland fire on a North American temperate peatland. *Fire Ecol.* **2017**, *13*, 34–57. [[CrossRef](#)]
4. Watts, A.C.; Kobziar, L.N. Smoldering combustion and ground fires: Ecological effects and multi-scale significance. *Fire Ecol.* **2013**, *9*, 124–132. [[CrossRef](#)]
5. Turetsky, M.R.; Benscoter, B.; Page, S.; Rein, G.; van der Werf, G.R.; Watts, A. Global vulnerability of peatlands to fire and carbon loss. *Nat. Geosci.* **2015**, *8*, 11–14. [[CrossRef](#)]
6. Blauw, L.G.; van Logtestijn, R.S.P.; Broekman, R.; Aerts, R.; Cornelissen, J.H.C. Tree species identity in high-latitude forests determines fire spread through fuel ladders from branches to soil and vice versa. *For. Ecol. Manag.* **2017**, *400*, 475–484. [[CrossRef](#)]
7. Evtyugina, M.; Calvo, A.I.; Nunes, T.; Alves, C.; Fernandes, A.P.; Tarelho, L.; Vicente, A.; Pio, C. VOC emissions of smouldering combustion from Mediterranean wildfires in central Portugal. *Atmos. Environ.* **2013**, *64*, 339–348. [[CrossRef](#)]
8. Brown, E.K.; Wang, J.; Feng, Y. US wildfire potential: A historical view and future projection using high-resolution climate data. *Environ. Res. Lett.* **2020**, *16*, 034060. [[CrossRef](#)]
9. Kuklina, V.; Sizov, O.; Rasputina, E.; Bilichenko, I.; Krasnoshtanova, N.; Bogdanov, V.; Petrov, A.N. Fires on ice: Emerging permafrost peatlands fire regimes in Russia’s subarctic taiga. *Land* **2022**, *11*, 322. [[CrossRef](#)]
10. Carroll, R.; Wright, I.A.; Reynolds, J.K. Loss of soil carbon in a world heritage peatland following a bushfire. *Int. J. Wildland Fire* **2023**, *32*, 1059–1070. [[CrossRef](#)]
11. Wilkinson, S.L.; Andersen, R.; Moore, P.A.; Davidson, S.J.; Granath, G.; Waddington, J.M. Wildfire and degradation accelerate northern peatland carbon release. *Nat. Clim. Chang.* **2023**, *13*, 456–461. [[CrossRef](#)]
12. Xifré-Salvadó, M.À.; Prat-Guitart, N.; Francos, M.; Úbeda, X.; Castellnou, M. Smouldering combustion dynamics of a soil from a pinus halepensis mill. Forest. A case study of the rocallaura fires in northeastern Spain. *Appl. Sci.* **2020**, *10*, 3449. [[CrossRef](#)]
13. Marcotte, A.L.; Limpens, J.; Stoof, C.R.; Stoorvogel, J.J. Can ash from smoldering fires increase peatland soil pH? *Int. J. Wildland Fire* **2022**, *31*, 607–620. [[CrossRef](#)]
14. Dellasala, D.A.; Williams, J.E.; Williams, C.D.; Franklin, J.F. Beyond smoke and mirrors: A synthesis of fire policy and science. *Conserv. Biol.* **2004**, *18*, 976–986. [[CrossRef](#)]
15. Hadden, R.M.; Rein, G.; Belcher, C.M. Study of the competing chemical reactions in the initiation and spread of smouldering combustion in peat. *Proc. Combust. Inst.* **2013**, *34*, 2547–2553. [[CrossRef](#)]
16. Chen, H.; Rein, G.; Liu, N. Numerical investigation of downward smoldering combustion in an organic soil column. *Int. J. Heat Mass Transf.* **2015**, *84*, 253–261. [[CrossRef](#)]
17. Huang, X.; Rein, G. Upward-and-downward spread of smoldering peat fire. *Proc. Combust. Inst.* **2019**, *37*, 4025–4033. [[CrossRef](#)]
18. Nyman, P.; Metzen, D.; Noske, P.J.; Lane, P.N.J.; Sheridan, G.J. Quantifying the effects of topographic aspect on water content and temperature in fine surface fuel. *Int. J. Wildland Fire* **2015**, *24*, 1129–1142. [[CrossRef](#)]
19. Magdić, I.; Safner, T.; Rubinić, V.; Rutić, F.; Husnjak, S.; Filipović, V. Effect of slope position on soil properties and soil moisture regime of Stagnosol in the vineyard. *J. Hydrol. Hydromech.* **2022**, *70*, 62–73. [[CrossRef](#)]
20. Asensio, M.I.; Ferragut, L. On a wildland fire model with radiation. *Int. J. Numer. Methods Eng.* **2002**, *54*, 137–157. [[CrossRef](#)]
21. Morandini, F.; Silvani, X.; Dupuy, J.-L.; Susset, A. Fire spread across a sloping fuel bed: Flame dynamics and heat transfers. *Combust. Flame* **2018**, *190*, 158–170. [[CrossRef](#)]

22. Rossa, C.G.; Davim, D.A.; Viegas, D.X. Behaviour of slope and wind backing fires. *Int. J. Wildland Fire* **2015**, *24*, 1085–1097. [[CrossRef](#)]
23. Abouali, A.; Viegas, D.X.; Raposo, J.R. Analysis of the wind flow and fire spread dynamics over a sloped–ridgeline hill. *Combust. Flame* **2021**, *234*, 111724. [[CrossRef](#)]
24. Rodrigues, A.; Ribeiro, C.; Raposo, J.; Viegas, D. X.; André, J. Effect of canyons on a fire propagating laterally over slopes. *Front. Mech. Eng.* **2019**, *5*, 41.
25. Guo, H.; Xiang, D.; Kong, L.; Gao, Y.; Zhang, Y. Upslope fire spread and heat transfer mechanism over a pine needle fuel bed with different slopes and winds. *Appl. Therm. Eng.* **2023**, *229*, 120605. [[CrossRef](#)]
26. Santoso, M.A.; Christensen, E.G.; Yang, J.; Rein, G. Review of the transition from smouldering to flaming combustion in wildfires. *Front. Mech. Eng.* **2019**, *5*, 49. [[CrossRef](#)]
27. Reardon, J.; Hungerford, R.; Ryan, K. Factors affecting sustained smouldering in organic soils from pocosin and pond pine woodland wetlands. *Int. J. Wildland Fire* **2007**, *16*, 107–118. [[CrossRef](#)]
28. Reardon, J.J.; Curcio, G.M. Estimated smoldering probability: A new tool for predicting ground fire in the organic soils on the North Carolina Coastal Plain. *Fire Manag. Today* **2011**, *4*, 95–104.
29. Schulte, M.L.; McLaughlin, D.L.; Wurster, F.C.; Varner, J.M.; Stewart, R.D.; Aust, W.M.; Jones, C.N.; Gile, B. Short-and long-term hydrologic controls on smouldering fire in wetland soils. *Int. J. Wildland Fire* **2019**, *28*, 177–186. [[CrossRef](#)]
30. Wang, Z.; Lai, C.; Chen, X.; Yang, B.; Zhao, S.; Bai, X. Flood hazard risk assessment model based on random forest. *J. Hydrol.* **2015**, *527*, 1130–1141. [[CrossRef](#)]
31. Woolford, D.G.; Martell, D.L.; McFayden, C.B.; Evens, J.; Stacey, A.; Wotton, B.M.; Boychuk, D. The development and implementation of a human-caused wildland fire occurrence prediction system for the province of Ontario, Canada. *Can. J. For. Res.* **2021**, *51*, 303–325. [[CrossRef](#)]
32. Pang, Y.; Li, Y.; Feng, Z.; Feng, Z.; Zhao, Z.; Chen, S.; Zhang, H. Forest fire occurrence prediction in China based on machine learning methods. *Remote Sens.* **2022**, *14*, 5546. [[CrossRef](#)]
33. Singh, M.; Huang, Z. Analysis of forest fire dynamics, distribution and main drivers in the Atlantic Forest. *Sustainability* **2022**, *14*, 992. [[CrossRef](#)]
34. Wang, W.; Zhao, F.; Wang, Y.; Huang, X.; Ye, J. Seasonal differences in the spatial patterns of wildfire drivers and susceptibility in the southwest mountains of China. *Sci. Total Environ.* **2023**, *869*, 161782. [[CrossRef](#)] [[PubMed](#)]
35. Tuyen, T.T.; Jaafari, A.; Yen, H.P.H.; Nguyen-Thoi, T.; Phong, T.V.; Nguyen, H.D.; Le, H.V.; Phuong, T.T.M.; Nguyen, S.H.; Prakash, I.; et al. Mapping forest fire susceptibility using spatially explicit ensemble models based on the locally weighted learning algorithm. *Ecol. Inform.* **2021**, *63*, 101292. [[CrossRef](#)]
36. Iban, M.C.; Sekertekin, A. Machine learning based wildfire susceptibility mapping using remotely sensed fire data and GIS: A case study of Adana and Mersin provinces, Turkey. *Ecol. Inform.* **2022**, *69*, 101647. [[CrossRef](#)]
37. Trucchia, A.; Meschi, G.; Fiorucci, P.; Gollini, A.; Negro, D. Defining wildfire susceptibility maps in Italy for understanding seasonal wildfire regimes at the national level. *Fire* **2022**, *5*, 30. [[CrossRef](#)]
38. Radandima, G.U.E.R. I Identification of Land Fire Risk Areas with Random Forest Using Landsat Image Data 8 OLI. *Int. J. Nat. Sci. Eng.* **2022**, *6*, 64–74. [[CrossRef](#)]
39. Li, X.; Zhang, G.; Tan, S.; Yang, Z.; Wu, X. Forest Fire Smoke Detection Research Based on the Random Forest Algorithm and Sub-Pixel Mapping Method. *Forests* **2023**, *14*, 485. [[CrossRef](#)]
40. Sathishkumar, V.E.; Cho, J.; Subramanian, M.; Naren, O.S. Forest fire and smoke detection using deep learning-based learning without forgetting. *Fire Ecol.* **2023**, *19*, 9. [[CrossRef](#)]
41. Davies, G.M.; Gray, A.; Rein, G.; Legg, C.J. Peat consumption and carbon loss due to smouldering wildfire in a temperate peatland. *For. Ecol. Manag.* **2013**, *308*, 169–177. [[CrossRef](#)]
42. Lin, S.; Liu, Y.; Huang, X. How to build a firebreak to stop smouldering peat fire: Insights from a laboratory-scale study. *Int. J. Wildland Fire* **2021**, *30*, 454–461. [[CrossRef](#)]
43. Rein, G.; Cleaver, N.; Ashton, C.; Pironi, P.; Torero, J.L. The severity of smouldering peat fires and damage to the forest soil. *Catena* **2008**, *74*, 304–309. [[CrossRef](#)]
44. Zhang, H.; Guo, P.; Chen, H.; Liu, N.; Qiao, Y.; Xu, M.; Zhang, L. Lightning-induced smoldering ignition of peat: Simulation experiments by an electric arc with long continuing current. *Proc. Combust. Inst.* **2023**, *39*, 4185–4193. [[CrossRef](#)]
45. Liu, Y.; Trancoso, R.; Ma, Q.; Ciais, P.; Gouvêa, L.P.; Yue, C.; Assis, J.; Blanco, J.A. Carbon density in boreal forests responds non-linearly to temperature: An example from the Greater Khingan Mountains, northeast China. *Agric. For. Meteorol.* **2023**, *338*, 109519. [[CrossRef](#)]
46. Lin, S.; Huang, X. Quenching of smoldering: Effect of wall cooling on extinction. *Proc. Combust. Inst.* **2021**, *38*, 5015–5022. [[CrossRef](#)]
47. Cancellieri, D.; Leroy-Cancellieri, V.; Leoni, E.; Simeoni, A.; Kuzin, A.Y.; Filkov, A.I.; Rein, G. Kinetic investigation on the smouldering combustion of boreal peat. *Fuel* **2012**, *93*, 479–485. [[CrossRef](#)]
48. Huang, X.; Rein, G. Smouldering combustion of peat in wildfires: Inverse modelling of the drying and the thermal and oxidative decomposition kinetics. *Combust. Flame* **2014**, *161*, 1633–1644. [[CrossRef](#)]
49. Lu, Z. A diffusion-flame analog of forward smolder waves:(I) 1-D steady structures. *Combust. Flame* **2018**, *196*, 515–528. [[CrossRef](#)]

50. Prat-Guitart, N.; Rein, G.; Hadden, R.M.; Belcher, C.M.; Yearsley, J.M. Effects of spatial heterogeneity in moisture content on the horizontal spread of peat fires. *Sci. Total Environ.* **2016**, *572*, 1422–1430. [[CrossRef](#)]
51. Lin, S.; Cheung, Y.K.; Xiao, Y.; Huang, X. Can rain suppress smoldering peat fire? *Sci. Total Environ.* **2020**, *727*, 138468. [[CrossRef](#)]
52. Ohlemiller, T.J. Modeling of smoldering combustion propagation. *Prog. Energy Combust. Sci.* **1985**, *11*, 277–310. [[CrossRef](#)]
53. Graham, L.L.B.; Applegate, G.B.; Thomas, A.; Ryan, K.C.; Saharjo, B.H.; Cochrane, M.A. A field study of tropical peat fire behaviour and associated carbon emissions. *Fire* **2022**, *5*, 62. [[CrossRef](#)]
54. Ribeiro, C.; Viegas, D.X.; Raposo, J.; Reis, L.; Sharples, J. Slope effect on junction fire with two non-symmetric fire fronts. *Int. J. Wildland Fire* **2023**, *32*, 328–335. [[CrossRef](#)]
55. Pimont, F.; Dupuy, J.-L.; Linn, R. Coupled slope and wind effects on fire spread with influences of fire size: A numerical study using FIRETEC. *Int. J. Wildland Fire* **2012**, *21*, 828–842. [[CrossRef](#)]
56. Liu, N.; Wu, J.; Chen, H.; Xie, X.; Zhang, L.; Yao, B.; Zhu, J.; Shan, Y. Effect of slope on spread of a linear flame front over a pine needle fuel bed: Experiments and modelling. *Int. J. Wildland Fire* **2014**, *23*, 1087–1096. [[CrossRef](#)]
57. Guo, F.; Wang, G.; Su, Z.; Liang, H.; Wenhui, W.; Lin, F.; Liu, A. What drives forest fire in Fujian, China? Evidence from logistic regression and Random Forests. *Int. J. Wildland Fire* **2016**, *25*, 505–519. [[CrossRef](#)]
58. Milanović, S.; Marković, N.; Pamučar, D.; Gigovic, L.; Kostic, P.; Milanović, S.D. Forest Fire Probability Mapping in Eastern Serbia: Logistic Regression versus Random Forest Method. *Forests* **2020**, *12*, 5. [[CrossRef](#)]
59. Eslami, R.; Azarnoush, M.R.; Kialashki, A.; Kazemzadeh, F. GIS-based forest fire susceptibility assessment by random forest, artificial neural network and logistic regression methods. *J. Trop. For. Sci.* **2021**, *33*, 173–184. [[CrossRef](#)]
60. Gigovic, L.; Pourghasemi, H.R.; Drobnyak, S.; Bai, S. Testing a New Ensemble Model Based on SVM and Random Forest in Forest Fire Susceptibility Assessment and Its Mapping in Serbia's Tara National Park. *Forests* **2019**, *10*, 408. [[CrossRef](#)]
61. Elia, M.; D'Este, M.; Ascoli, D.; Giannico, V.; Spano, G.; Ganga, A.; Colangelo, G.; Laforteza, R.; Sanesi, G. Estimating the probability of wildfire occurrence in Mediterranean landscapes using Artificial Neural Networks. *Environ. Impact Assess. Rev.* **2020**, *85*, 106474. [[CrossRef](#)]

Disclaimer/Publisher's Note: The statements, opinions and data contained in all publications are solely those of the individual author(s) and contributor(s) and not of MDPI and/or the editor(s). MDPI and/or the editor(s) disclaim responsibility for any injury to people or property resulting from any ideas, methods, instructions or products referred to in the content.